HHS Public Access

Author manuscript

Anal Biochem. Author manuscript; available in PMC 2018 July 15.

Published in final edited form as:

Anal Biochem. 2017 July 15; 529: 171–178. doi:10.1016/j.ab.2016.08.026.

In Vivo ^{17}O MRS Imaging – Quantitative Assessment of Regional Oxygen Consumption and Perfusion Rates in Living Brain

Xiao-Hong Zhu and **Wei Chen**

Center for Magnetic Resonance Research, Department of Radiology, University of Minnesota, School of Medicine, Minneapolis, MN

Abstract

In the last decade, *in vivo* oxygen-17 (^{17}O) MRS has evolved into a promising MR technique for noninvasively studying oxygen metabolism and perfusion in aerobic organs with the capability of imaging the regional metabolic rate of oxygen and its changes. In this chapter, we will briefly review the methodology of the *in vivo* ^{17}O MRS technique and its recent development and applications; we will also discuss the advantages of the high/ultrahigh magnetic field for ^{17}O MR detection, as well as the challenges and potential of this unique MRS method for biomedical research of oxygen metabolism, mitochondrial function and tissue energetics in health and disease.

Introduction

Compared to well-established *in vivo* magnetic resonance (MR) spectroscopy (MRS) methodologies such as phosphrous-31 (^{31}P) or carbon-13 (^{13}C) MRS [1], *in vivo* oxygen-17 (^{17}O) MRS has had a relatively short history and is less commonly employed in biomedical research. As one of the most abundant elements on earth, molecules containing oxygen exist in all forms and levels of life. Thus, efforts to develop and utilize ^{17}O-based MR technology to obtain valuable information of biological systems are ongoing. Perhaps the most intriguing use of *in vivo* ^{17}O MRS is to study the cellular oxygen metabolism in living organs. The original idea to use ^{17}O MRS for *in vivo* studies appeared in the late 1980s [2–7], and it was likely inspired by the ^{15}O-based positron emission tomography (PET) technique developed for imaging the cerebral metabolic rate of oxygen ($CMRO_2$), a critically important physiological parameter of the brain [8, 9].

Among all neuroimaging modalities capable of providing $CMRO_2$ information, ^{15}O-PET has been regarded as a gold standard for directly imaging the oxygen metabolic rate in the living brain. However, two major drawbacks associated with ^{15}O-PET imaging have seriously limited its availability and applicability: one is the very short half-life of ^{15}O (2.04 min), which requires expensive equipment such as a cyclotron to produce the ^{15}O-tracers on site; and the other is the inability of the ^{15}O-PET in distinguishing the ^{15}O signals of the oxygen substrate from that of metabolically produced water, so additional measurements and

complicated mathematical models are needed to calculate the $CMRO_2$ values [8, 9]. Magnetic resonance technology is a widely used neuroimaging modality in present-day medical research and clinical practice. ^{17}O MRS (or imaging) and ^{1}H MRI-based approaches have been developed for assessing $CMRO_2$. Even though the ^{17}O-MR approach is technically much simpler than ^{15}O-PET since it only detects the metabolically generated water signal (see details below) and does not require the injection of large radiation doses to the subject, its initial utilization was slow, with only a small number of publications in the first decade after inception that mainly focused on feasibility assessment [10–16]. The major challenge in advancing this technology can be attributed to the extremely low intrinsic sensitivity of ^{17}O as compared to that of ^{1}H (~1×10^5 fold differences) at natural abundance [17]. On the other hand, ^{1}H MRI detects abundant water signals with great sensitivity, although the water signals in general cannot be directly related to oxygen metabolism. To specifically assess cerebral oxygenation, several methods based on ^{1}H MRI have been introduced [18–23]. They include (i) the blood oxygenation level dependent (BOLD) functional magnetic resonance imaging (fMRI) in combination with hypercapnic and hyperoxic respiratory challenges to calibrate the fMRI signals [19, 21]; (ii) susceptometry-based or T_2-based methods to determine the cerebral venous oxygen saturation (Yv) [22, 23]; and (iii) a quantitative BOLD approach to extract the venous cerebral blood volume (CBV) and deoxyhemoglobin concentration from the transverse relaxation time (T_2 or T_2^*) [18, 20]. However, these indirect methods have their own technical challenges and limitations; and various assumptions, predetermined parameters and different models must be applied in estimating $CMRO_2$.

High/ultrahigh field MR scanner technology emerged in the 1990s and the extraordinary sensitivity gain of ^{17}O detection at higher field observed in 2001 have stimulated new interests and efforts in the field of *in vivo* ^{17}O MRS research [24, 25]. After more than ten years of technology development and validation, the *in vivo* ^{17}O MRS/MRI methodology has now been established as a valuable tool for studying cerebral oxygen metabolism in preclinical animal models and in human brains under various physiopathological conditions [25–39]. Details of the technology development can be found in several earlier review articles [40–43]. In the present review, we will briefly describe the methodology and its utility for non-invasive investigation and quantitative understanding of the roles of oxygen metabolism in health and disease. The main scope of this review will be on the new advancements and recent applications in this research field.

Methodology Overview

Among the three stable isotopes of oxygen (i.e., ^{16}O, ^{17}O and ^{18}O), ^{16}O represents over 99.7% of the composition, but unfortunately does not possess a nuclear spin; only ^{17}O with a spin number of I=5/2 can be detected by MR. In this section, we will introduce different *in vivo* ^{17}O MR methods according to their signal sources and/or related uses with either a spectroscopic or imaging approach,.

Steady-state detection of the natural abundance ^{17}O signal

The relative amount of ^{17}O in oxygen in nature is very rare (only 0.037% of total oxygen). Because the concentration of major metabolites is in the range of few millimolar to tens millimolar, long ^{17}O MR acquisition times are required to accumulate reasonable signal for meaningful detection or adequate signal-to-noise ratio (SNR) of oxygen-containing metabolites in tissue samples. Figure 1 illustrates natural abundance *in vivo* ^{17}O MR spectra obtained in live and postmortem rat brains with a 11.7T scanner that required several million scans over 6 and 14 hours, respectively, in which a number of broad resonances from oxygen in phosphate, sulfonic and carbonyl groups covering a wide chemical shift range are detected [44]. It is clear that the SNR of these natural abundance ^{17}O signals is insufficient for practical applications aiming to monitor oxygen-containing metabolites. The only molecule that can be easily detected by *in vivo* ^{17}O MRS techniques is water, a major component of the tissue. However, with known water content and molar concentration in different tissues, the natural abundance water signal in ^{17}O MR spectra can serve as an internal reference for quantification purposes. This is an important advantage of the *in vivo* ^{17}O MR methodology a

Dynamic monitoring of the metabolism of ^{17}O-labled oxygen gas

A unique feature of the *in vivo* ^{17}O MR technique is its ability to directly and quantitatively monitor the production of metabolic water after the introduction of ^{17}O-labeled oxygen ($^{17}O_2$) gas to an animal or human. It is well known that when oxygen $^{17}O_2$ molecules enter the blood stream, they are brought to the organ or tissue of interest *via* effective blood circulation and perfusion. At the cellular level, the oxygen consumption occurs in the mitochondria through cellular respiration that generate ^{17}O-labeled water ($H_2{}^{17}O$); the rate of $H_2{}^{17}O$ production reflects the oxygen consumption rate. Since the $^{17}O_2$ molecules that are either bound to hemoglobin or dissolved in blood are invisible to ^{17}O MR detection, only $H_2{}^{17}O$ molecules, the final product of the oxygen metabolism, has an ^{17}O signal; therefore, dynamic *in vivo* ^{17}O MR measurements can be used to monitor the production of $H_2{}^{17}O$ and determine the metabolic rate of oxygen in the targeted tissue or organ. The principle of this technique, the quantification model and corresponding mass balance equation, as well as the simplified method for determining $CMRO_2$ and cerebral blood flow (CBF) in small animal brains *via* a brief (few minutes) inhalation of $^{17}O_2$ gas, are schematically illustrated in Figure 2; the detailed methodology and its validity, which has been experimentally verified in rat brains, can be found elsewhere [26, 29, 31, 34, 38–42].

Blood flow measurement with exogenous tracer of $H_2{}^{17}O$

Introducing ^{17}O-labeled water as an exogenous tracer and using dynamic *in vivo* ^{17}O MR technique to monitor the evolution of the $H_2{}^{17}O$ signal in targeted tissue or organ enables the determination of the washout rate of the $H_2{}^{17}O$ tracer, which represents the blood flow or perfusion rate [26, 31]. This approach is the same as conventional tracer techniques used in biomedical research or in the clinic. The ideal method of introducing $H_2{}^{17}O$ tracer is *via* a bolus injection to a feeding artery (e.g. the internal carotid artery) as shown in Figure 3 for CBF measurement, which is straightforward for CBF quantification but requires invasive procedures to gain access to the desired artery [26, 31]. Alternatively, intravenous injection

is less invasive and more common for human application, but the CBF quantification is more complicated and requires the tracer input function.

The use of metabolic $H_2{}^{17}O$ as an endogenous tracer for CBF measurement

The ^{17}O MR signal of the metabolic water generated in the mitochondria following a $^{17}O_2$ inhalation can serve as a perfusion tracer, and its decay rate (k) can be used to determine the CBF value with an experimentally derived correction factor (i.e., CBF ≈ 1.86 × k). This empirical approach was demonstrated in rat brains across a wide range of conditions [39]. This finding suggests that the dynamic *in vivo* ^{17}O MR technique is capable of simultaneously and noninvasively determining both $CMRO_2$ and CBF as schematically shown in Figure 2. Thus, ^{17}O MR provides a new method for studying the cerebral oxygen metabolism and perfusion underlying brain function and disease. In addition, the oxygen extraction fraction (OEF) that reflects the balance between oxygen supply and usage can be calculated from the corresponding $CMRO_2$ and CBF values using the relationship of $OEF = CMRO_2/(C_{a,O2}\times CBF)$, where $C_{a,O2}$ is a constant representing the arterial oxygen concentration of the brain [38]. Therefore, by combining the dynamic *in vivo* ^{17}O MR technique with a short $^{17}O_2$ gas inhalation, it is possible to quantify three important physiological parameters, namely $CMRO_2$, CBF and OEF in a completely non-invasive manner. A similar approach and quantification model in human brain has recently been developed [45].

In vivo ^{17}O MRS imaging (or MRI)

Another important feature of the *in vivo* ^{17}O MR technology is its capability of detecting not only the dynamic change of the ^{17}O signal but also the signal distribution in space via three-dimensional (3D) ^{17}O MRS imaging [41, 42] or MRI approaches, although conventional MRI sequences are not applicable due to the extremely short T_2 relaxation time of the $H_2{}^{17}O$ water (in the range of few milliseconds) [25, 28, 46, 47]. Thus, with this technique, it is possible to assess regional oxygen consumption and perfusion rates in the living brain or in other organs. Furthermore, after introducing an exogenous ^{17}O-tracer, the ^{17}O signal can reach a new steady state within a reasonable time window, e.g. ~10–20 minutes in the brain, which permits repeated measurements with subsequent tracer administration under different conditions [34]. This approach enables the quantification of the same parameter with absolute values at different states, as well as the changes due to altered physiological conditions or brain states [34, 35, 48].

The aforementioned methodological aspects of the *in vivo* ^{17}O MR technology reveal its unique utility for biomedical research in the area of oxygen metabolism, energetics and vascular-metabolic relationships in a living organ. It should be noted that the spatial and temporal resolution of dynamic ^{17}O MR imaging are dependent upon the available ^{17}O signal; thus, ^{17}O sensitivity is the key limiting factor that determines the spatial/temporal resolution and the reliability of the ^{17}O MR imaging.

Advantage of high/ultrahigh fields for *in vivo* ^{17}O MR imaging

^{17}O has a roughly 7 times lower gyromagnetic ratio and 2700 times lower natural abundance than ^{1}H, which leads to 10^5 times lower sensitivity compared to ^{1}H [17, 42]. The advantage of the high/ultrahigh magnetic field strength for improving the sensitivity of the ^{17}O MR imaging is essential for its potential applications. Such an advantage stems from the quadrupolar relaxation mechanism of the ^{17}O-water. The nearly field-independent relaxation times of the ^{17}O-water eliminates the potential signal loss commonly occurring in the ^{1}H MRS or MRI at higher field because increasing field strength will *not* prolong the longitudinal relaxation time (T_1) and/or shorten the T_2 (or T_2^*) of the ^{17}O-water. Thus, the acquisition efficiency of the ^{17}O MR signal will *not* be compromised [25, 28, 46, 47]. The extremely short T_1 of the ^{17}O-water permits fast acquisition and more signal averaging in unit sample time, thus enhancing the apparent ^{17}O SNR. Also, the effect of the magnetic field (B_0) inhomogeneity on the ^{17}O-water linewidth, which is inversely proportional to the T_2^*, is very small (negligible) compared to the effect of the quadrupolar relaxation [25, 28, 46, 47]. Therefore, *in vivo* ^{17}O MR measurement is virtually insensitive to the B_0 shimming, a challenging procedure faced by many other *in vivo* MRS methodologies.

The field-dependent relationship between the apparent ^{17}O-SNR (normalized to that of 9.4T) and the field strength across a wide B_0 range from zero up to 16.4T that was obtained from rat brains is displayed in Figure 4. The reported SNR increase with field strength is based on the empirical relationship of SNR $\approx C \times B_0^{\beta}$ with $C = 0.015$ and $\beta = 1.9$. This value of β is slightly higher than the theoretical prediction ($\beta = 1.75$) based on the work of Hoult et al. [49]; this could be due to imperfect control of the experimental variables (e.g. the Q factor (quality factor) of the radio frequency (RF) coils is not identical at different fields) used in the two studies. The finding of field-dependent ^{17}O-SNR enhancement suggests that compared to *in vivo* ^{1}H, ^{31}P and ^{13}C MRS methodologies, the *in vivo* ^{17}O MRS can benefit the most from the sensitivity gain at high/ultrahigh field strengths [46].

Recent development and applications of *in vivo* ^{17}O MRS and imaging

Preclinical study in animal brain

As noted above, currently, the *in vivo* ^{17}O MR methodology has been established for the simultaneous dynamic imaging of three important physiological parameters, namely $CMRO_2$, CBF and OEF in preclinical animal brain. An example of such a study is mouse brain, in which the animals have undergone transit middle cerebral arterial occlusion (tMCAo) (Figure 5). The figure displays anatomic regions of post-stroke brains with voxels located in ischemic and intact hemispheres, corresponding to dynamic $H_2{}^{17}O$ signals before, during and after 2-min $^{17}O_2$ inhalation; reproducibility between two repeated imaging measurements in the same animal; and the results of $CMRO_2$, CBF and OEF imaging indicate significant changes in the ischemia affected brain region [38]. This study demonstrates a promising ^{17}O-MR based imaging technique with the merits of robustness, simplicity, noninvasiveness and reliability, features that are essential for imaging abnormal oxygen metabolism and perfusion in diseased brains.

Several animal species commonly used in preclinical studies have been tested, which include mouse, rat, cat and swine at field strengths from 3T up to 16.4T; the results confirm the feasibility of dynamic *in vivo* ^{17}O MRS imaging for studying oxygen metabolism in these preclinical models [35, 38, 39, 48, 50–52]. This novel ^{17}O-MR based $CMRO_2$ imaging technique has been successfully applied to Huntington disease mouse brains and used as a metabolic imaging tool to assess the mitochondrial function in diseased brain *in vivo* by directly determining the cerebral oxygen consumption deficit under metabolic stress [51]. It is expected that more studies of this kind will be forthcoming once the research community recognizes the promise of this new technology.

Translational study in human brain

The dynamic *in vivo* ^{17}O MRS imaging approach can be easily applied to the human brain to monitor the change of $H_2{}^{17}O$ signals during and after a short $^{17}O_2$ inhalation [32]. However, to calculate the oxygen consumption rate from the dynamic $H_2{}^{17}O$ signals, the simplified model used in small animals is not suitable due to the slower exchange of the ^{17}O-labeled oxygen gas in the human body.

A three-phase model has been proposed, in which the time-dependent function of the ^{17}O-labeled oxygen gas fraction in arterial blood is modeled based on an estimated replacement rate of fresh ^{17}O-oxygen in the blood. In addition, two rate constants of K_L and K_G representing the loss and gain of $H_2{}^{17}O$ within the imaging voxel, respectively, are included in the proposed quantification model, whereas the CBF is not presented in the model since its influence on the measured signal is accounted for by the rate constants K_L and K_G [36]. Figure 6 shows results of human brain $CMRO_2$ mapping at 9.4T and two representative $H_2{}^{17}O$ time-courses in voxels with low and high metabolic rates. The model provides reasonable fitting to the ^{17}O MR data yielding regional $CMRO_2$ values with corresponding K_G and K_L constants [36].

Recently, a modified quantification model was proposed for human application. In this model, the exchange function of the ^{17}O-labeled oxygen in the human lung is accounted for by its influence on the fractional change of $^{17}O_2$ in the arterial blood. The $^{17}O_2$ gas exchange rate can be experimentally determined from a simple breathing test using non-labeled oxygen gas [45, 53]. This additional step is necessary for short $^{17}O_2$ inhalation because the transition of the oxygen gas in human lung takes ~2 min or longer to reach a steady state. More importantly, not only is it possible to obtain the $CMRO_2$ value, but the CBF value can also be obtained from the model fitting of the dynamic $H_2{}^{17}O$ signals in the human brain tissue. Consequently, all three parameters of $CMRO_2$, CBF and OEF can be simultaneously determined from the non-invasive ^{17}O MRS imaging measurement in humans with a $^{17}O_2$ inhalation as short as 2–3 min [45, 53].

Feasibility assessments in normal human brain at resting or functional stimulated state, and in diseased human brains were performed at a field strength of 3T up to 9.4T; the results are encouraging, indicating that the *in vivo* ^{17}O MRS imaging technique has the potential to become a promising neuroimaging modality for the translational study of oxygen metabolism in humans [45, 53–56]. It is worth pointing out, however, that future prospects

of this methodology will be largely affected by the challenges encountered in expanding this research field for routine applications at clinical settings (see more discussion later).

Study of oxygen metabolism in extracerebral tissues

Besides the brain, the heart is another highly aerobic organ consuming a large amount of oxygen since the oxygen metabolism is essential for supporting the mechanical work of myocyte contractions. The feasibility of applying the *in vivo* ^{17}O MR technique to hearts has been tested in rats at 9.4T [37, 57] and in human hearts at 3T [54]. The preliminary results as displayed in Figure 7 suggest that it is feasible to establish a noninvasive imaging modality with *in vivo* ^{17}O MR detection and appropriate quantification modeling for simultaneously imaging the myocardial oxygen metabolic rate (MVO_2) and myocardial perfusion [37].

Challenges and the potential of the *in vivo* ^{17}O MRS and imaging

The most important application of the *in vivo* ^{17}O MRS is to non-invasively study the oxygen metabolism in living animals or humans with introduction of $^{17}O_2$ gas. A major obstacle in this regard is the relatively high cost due to the limited supply of the ^{17}O-enriched oxygen gas. Currently, only few vendors can provide ^{17}O-isotope-labeled oxygen gas in large quantities with high enrichment, while the demand for this oxygen isotope is also limited. Increasing the demand may stimulate ^{17}O-oxygen production and lower its cost; but at present, saving the cost by reducing or improving the efficiency of the ^{17}O-oxygen gas usage seems to be the main focus, which is particularly crucial for human studies. Rebreathing pure $^{17}O_2$ with the CO_2 removed from the expired gas [36], and using a demand oxygen delivery system to reduce the total $^{17}O_2$ gas supply [55, 56] and/or recycling the expired $^{17}O_2$ gas for animal studies [32, 45, 53] are a few approaches being explored for this purpose. An alternative approach that administers $^{17}O_2$-enriched blood substitutes instead of $^{17}O_2$ inhalation has been suggested with the assumption that the high oxygen affinity of the artificial blood would improve its delivery efficiency [43, 58]; although the effectiveness and ability of this approach for accurately quantifying the metabolic rate of oxygen is yet to be determined. On the other hand, minimizing the $^{17}O_2$ gas inhalation time is a more effective way to lower the cost, although it requires a higher temporal resolution of the dynamic ^{17}O measurement.

Limited detection sensitivity is another major challenge encountered in the *in vivo* ^{17}O MR study. This is particularly critical for dynamic ^{17}O MR imaging since both spatial and temporal resolutions are key factors demanding high ^{17}O sensitivity. High/ultrahigh field scanners are employed in the ^{17}O MRS imaging studies due to the advantages in gain of sensitivity. It has been shown that a few millimeter spatial resolution in preclinical studies [26, 34, 35, 37–39, 48, 50, 51] and close to a centimeter in human studies [32, 45, 53] with ~10–15 sec temporal resolution can be reached with $B_0 \geq 7$T. Relatively lower resolutions are expected with lower field magnets, e.g., a 3T clinical scanner, or when large volume coils are employed [30, 36, 54, 56]. It is worth mentioning that while ^{17}O MR benefits from the sensitivity gain at a higher field, it also requires a larger RF power to achieve the same RF pulse flip angle because of its low γ-ratio. Interestingly, a recent study has found that the high RF power demand in the ^{17}O MR measurement is significantly compensated by its high

B_1 efficiency as compared to that of ^{1}H MR at high/ultrahigh fields [59]. Of course, for human application, the specific absorption rate (SAR) has to be closely monitored to ensure it is below the FDA guideline, which could limit our ability to optimize the ^{17}O MR acquisition parameters in the human studies.

Despite the limitation in the ^{17}O detection sensitivity, the apparent SNR (i.e., the SNR in unit acquisition time) of the ^{17}O MRS is still better than that of ^{1}H, ^{13}C and ^{31}P MRS, if the identical coil performance, acquisition scheme (e.g. at fully relaxed condition) and metabolite concentrations are used in comparison. Such unexpected superiority in sensitivity may be attributed to the relaxation times of the ^{17}O nucleus, which are extremely short (in the order of few milliseconds), thus allowing efficient signal averaging during acquisition. To further improve the spatial resolution of the ^{17}O-MR based $CMRO_2$ mapping, novel MR imaging techniques with efficient signal acquisition scheme and/or denoising capability are worthy of exploration [60].

In summary, after nearly three decades, *in vivo* ^{17}O MRS and imaging is slowly emerging as a promising MR technique for noninvasively studying oxygen metabolism and perfusion in aerobic organs with the capability of imaging regional metabolic rates of oxygen and its change; thus providing a valuable tool for biomedical research of oxygen metabolism, mitochondrial function and tissue energetics in health and disease.

Acknowledgments

The authors thank Drs. Byeong-Yuel Lee, Xiao Liu, Ming Lu, Kamil Ugurbil, Nanyin Zhang, Xiaoliang Zhang, Yi Zhang and Mr. John Strupp and Hannes Wiesner for their technical assistance and support. The reviewed work was partially funded by the NIH grants of NS041262, NS057560, NS070839, R24 MH106049, R24 MH106049-S1, P30 NS076408, P41 EB015894 and S10 RR026783; and the W.M. Keck Foundation.

Abbreviations

α	^{17}O enrichment fraction of inhaled $^{17}O_2$ gas
B_0	Magnetic field strength
BOLD	Blood oxygenation level dependent
$C_a(t)$	Time-dependent $H_2{}^{17}O$ concentration in excess of the natural abundance level in the arterial blood
$C_b(t)$	Time-dependent $H_2{}^{17}O$ concentration in excess of the natural abundance level in the brain tissue
$C_v(t)$	Time-dependent $H_2{}^{17}O$ concentration in excess of the natural abundance level in the venous blood
CBF	Cerebral blood flow
CBV	Cerebral blood volume
$CMRO_2$	Cerebral metabolic rate of oxygen

FDA	Food and Drug Administration (U.S.)
fMRI	Functional magnetic resonance imaging
$H_2{}^{17}O$	Oxygen-17 labeled water
k	Decay rate of the endogenous $H_2{}^{17}O$ tracer
K_L	Rate constants reflecting the loss of $H_2{}^{17}O$ within the imaging voxel
K_G	Rate constants reflecting the gain of $H_2{}^{17}O$ within the imaging voxel
λ	Brain-blood partition coefficient
MR	Magnetic resonance
MRI	Magnetic resonance imaging
MRS	Magnetic resonance spectroscopy
MVO_2	Myocardial oxygen metabolic rate
OEF	Oxygen extraction fraction
$^{17}O_2$	Oxygen-17 labeled oxygen gas
PET	Positron emission tomography
Q factor	Quality factor of the radio frequency coil
RF	Radio frequency
SAR	Specific absorption rate
SNR	Signal-to-noise ratio
T_1	Longitudinal relaxation time
T_2 (or T_2^*)	Transverse relaxation time (or apparent T_2)
tMCAo	Transit middle cerebral arterial occlusion
Yv	Cerebral venous oxygen saturation

References

1. Shulman RG, Brown TR, Ugurbil K, Ogawa S, Cohen SM, den Hollander JA. Cellular applications of ^{31}P and ^{13}C nuclear magnetic resonance. Science. 1979; 205:160–166. [PubMed: 36664]
2. Mateescu GD, Yvars GM, Dular T. Oxygen-17 Magnetic Resonance Imaging. Proc Inter Soc Magn Reson Med. 1987; 6:929.
3. Mateescu, GD., Yvars, GM., Dular, T. Water, Ions and O-17 Magnetic Resonance Imaging. In: Lauger, P.Packer, L., Vasilescu, V., editors. Water and Ions in Biological Systems. Birkhauser Verlag, Basel-Boston-Berlin; 1988. p. 239-250.

4. Mateescu GD, Yvars GM, Maylish-Kogovsek L, LaManna JC, Lust WD, Sudilovsky D. Oxygen-17 MRI and MRS of the brain, the heart and coronary arteries. Proc Inter Soc Magn Reson Med. 1989; 8:659.
5. Arai T, Nakao S, Mori K, Ishimori K, Morishima I, Miyazawa T, Fritz-Zieroth B. Cerebral oxygen utilization analyzed by the use of oxygen-17 and its nuclear magnetic resonance. Biochem Biophys Res Commun. 1990; 169:153–158. [PubMed: 2350339]
6. Arai T, Mori K, Nakao S, Watanabe K, Kito K, Aoki M, Mori H, Morikawa S, Inubushi T. In vivo oxygen-17 nuclear magnetic resonance for the estimation of cerebral blood flow and oxygen consumption. Biochem Biophys Res Commun. 1991; 179:954–961. [PubMed: 1898415]
7. Pekar J, Ligeti L, Ruttner Z, Lyon RC, Sinnwell TM, van Gelderen P, Fiat D, Moonen CT, McLaughlin AC. In vivo measurement of cerebral oxygen consumption and blood flow using ^{17}O magnetic resonance imaging. Magn Reson Med. 1991; 21:313–319. [PubMed: 1745131]
8. Mintun MA, Raichle ME, Martin WR, Herscovitch P. Brain oxygen utilization measured with O-15 radiotracers and positron emission tomography. J Nucl Med. 1984; 25:177–187. [PubMed: 6610032]
9. Ter-Pogossian MM, Eichling JO, Davis DO, Welch MJ. The measure in vivo of regional cerebral oxygen utilization by means of oxyhemoglobin labeled with radioactive oxygen-15. J Clin Invest. 1970; 49:381–391. [PubMed: 5411789]
10. Fiat D, Kang S. Determination of the rate of cerebral oxygen consumption and regional cerebral blood flow by non-invasive ^{17}O in vivo NMR spectroscopy and magnetic resonance imaging: Part 1. Theory and data analysis methods. Neurol Res. 1992; 14:303–311. [PubMed: 1360624]
11. Fiat D, Ligeti L, Lyon RC, Ruttner Z, Pekar J, Moonen CT, McLaughlin AC. In vivo ^{17}O NMR study of rat brain during $^{17}O_2$ inhalation. Magn Reson Med. 1992; 24:370–374. [PubMed: 1569875]
12. Fiat D, Dolinsek J, Hankiewicz J, Dujovny M, Ausman J. Determination of regional cerebral oxygen consumption in the human: ^{17}O natural abundance cerebral magnetic resonance imaging and spectroscopy in a whole body system. Neurol Res. 1993; 15:237–248. [PubMed: 8105403]
13. Fiat D, Kang S. Determination of the rate of cerebral oxygen consumption and regional cerebral blood flow by non-invasive ^{17}O in vivo NMR spectroscopy and magnetic resonance imaging. Part 2. Determination of $CMRO_2$ for the rat by ^{17}O NMR, and $CMRO_2$, rCBF and the partition coefficient for the cat by ^{17}O MRI. Neurol Res. 1993; 15:7–22. [PubMed: 8098859]
14. Mateescu GD, Fercu D. Concerted $^{17}O/^{31}P$ magnetic resonance spectroscopy: a novel approach for in vivo correlation of oxygen consumption and phosphate metabolism. Adv Exp Biol. 1994; 361:234.
15. Pekar J, Sinnwell T, Ligeti L, Chesnick AS, Frank JA, McLaughlin AC. Simultaneous measurement of cerebral oxygen consumption and blood flow using ^{17}O and ^{19}F magnetic resonance imaging. J Cereb Blood Flow Metab. 1995; 15:312–320. [PubMed: 7860664]
16. Mateescu GD, Cabrera ME. In vivo ^{17}O magnetic resonance spectroscopy. Determination of temperature effects on metabolic rates (Q10 factor). Adv Exp Med Biol. 1997; 411:585–590. [PubMed: 9269476]
17. Gerothanassis IP. Oxygen-17 NMR spectroscopy: Basic principles and applications (Part I). Progress in NMR Spectroscopy. 2010; 56:95–197.
18. An H, Lin W, Celik A, Lee YZ. Quantitative measurements of cerebral metabolic rate of oxygen utilization using MRI: a volunteer study. NMR Biomed. 2001; 14:441–447. [PubMed: 11746936]
19. Bulte DP, Kelly M, Germuska M, Xie J, Chappell MA, Okell TW, Bright MG, Jezzard P. Quantitative measurement of cerebral physiology using respiratory-calibrated MRI. Neuroimage. 2012; 60:582–591. [PubMed: 22209811]
20. Christen T, Bolar DS, Zaharchuk G. Imaging brain oxygenation with MRI using blood oxygenation approaches: methods, validation, and clinical applications, AJNR. American journal of neuroradiology. 2013; 34:1113–1123. [PubMed: 22859287]
21. Gauthier CJ, Hoge RD. Magnetic resonance imaging of resting OEF and $CMRO_2$ using a generalized calibration model for hypercapnia and hyperoxia. Neuroimage. 2012; 60:1212–1225. [PubMed: 22227047]

22. Jain V, Langham MC, Wehrli FW. MRI estimation of global brain oxygen consumption rate. J Cereb Blood Flow Metab. 2010; 30:1598–1607. [PubMed: 20407465]
23. Lu H, Ge Y. Quantitative evaluation of oxygenation in venous vessels using T_2-Relaxation-Under-Spin-Tagging MRI. Magn Reson Med. 2008; 60:357–363. [PubMed: 18666116]
24. Ugurbil K, Adriany G, Andersen P, Chen W, Garwood M, Gruetter R, Henry PG, Kim SG, Lieu H, Tkac I, Vaughan T, Van De Moortele PF, Yacoub E, Zhu XH. Ultrahigh field magnetic resonance imaging and spectroscopy. Magnetic resonance imaging. 2003; 21:1263–1281. [PubMed: 14725934]
25. Zhu XH, Merkle H, Kwag JH, Ugurbil K, Chen W. ^{17}O relaxation time and NMR sensitivity of cerebral water and their field dependence. Magn Reson Med. 2001; 45:543–549. [PubMed: 11283979]
26. Zhu XH, Zhang Y, Tian RX, Lei H, Zhang N, Zhang X, Merkle H, Ugurbil K, Chen W. Development of ^{17}O NMR approach for fast imaging of cerebral metabolic rate of oxygen in rat brain at high field. Proc Natl Acad Sci U S A. 2002; 99:13194–13199. [PubMed: 12242341]
27. Mateescu GD. Functional oxygen-17 magnetic resonance imaging and localized spectroscopy. Adv Exp Med Biol. 2003; 510:213–218. [PubMed: 12580430]
28. Thelwall PE, Blackband SJ, Chen W. Field dependence of ^{17}O T_1, T_2 and SNR – in vitro and in vivo studies at 4.7, 11 and 17.6 Tesla. Proc Intl Soc Mag Reson Med. 2003; 11:504.
29. Zhang X, Zhu XH, Tian R, Zhang Y, Merkle H, Chen W. Measurement of arterial input function of ^{17}O water tracer in rat carotid artery by using a region-defined (REDE) implanted vascular RF coil. Magma. 2003; 16:77–85. [PubMed: 12845538]
30. Fiat D, Hankiewicz J, Liu S, Trbovic S, Brint S. ^{17}O magnetic resonance imaging of the human brain. Neurol Res. 2004; 26:803–808. [PubMed: 15727263]
31. Zhang N, Zhu XH, Lei H, Ugurbil K, Chen W. Simplified methods for calculating cerebral metabolic rate of oxygen based on 17^O magnetic resonance spectroscopic imaging measurement during a short $^{17}O_2$ inhalation. J Cereb Blood Flow Metab. 2004; 24:840–848. [PubMed: 15362714]
32. Zhu XH, Zhang X, Zhang N, Zhang Y, Strupp J, Ugurbil K, Chen W. High-field ^{17}O Study of 3D $CMRO_2$ Imaging in human visual cortex. Proc Intl Soc Mag Reson Med. 2006; 14:409.
33. Zhu XH, Zhang Y, Chen W. Simultaneous and Ultrafast Monitoring of $CMRO_2$, CBF and pO_2 Changes in Response to Acute Global Ischemia in Rat Brain Proc. Intl Soc Mag Reson Med. 2007; 15:2393.
34. Zhu XH, Zhang Y, Zhang N, Ugurbil K, Chen W. Noninvasive and three-dimensional imaging of $CMRO_2$ in rats at 9.4 T: reproducibility test and normothermia/hypothermia comparison study. J Cereb Blood Flow Metab. 2007; 27:1225–1234. [PubMed: 17133228]
35. Zhu XH, Zhang N, Zhang Y, Ugurbil K, Chen W. New insights into central roles of cerebral oxygen metabolism in the resting and stimulus-evoked brain. J Cereb Blood Flow Metab. 2009; 29:10–18. [PubMed: 18781163]
36. Atkinson IC, Thulborn KR. Feasibility of mapping the tissue mass corrected bioscale of cerebral metabolic rate of oxygen consumption using 17-oxygen and 23-sodium MR imaging in a human brain at 9.4 T. Neuroimage. 2010; 51:723–733. [PubMed: 20188194]
37. Zhu XH, Zhang Y, Chen W. In Vivo ^{17}O MRS Imaging for Assessing Myocardial Oxygen Metabolism in Rat Heart at 9.4T. Proc Intl Soc Mag Reson Med. 2010; 18:172.
38. Zhu XH, Chen JM, Tu TW, Chen W, Song SK. Simultaneous and noninvasive imaging of cerebral oxygen metabolic rate, blood flow and oxygen extraction fraction in stroke mice. Neuroimage. 2013; 64:437–447. [PubMed: 23000789]
39. Zhu XH, Zhang Y, Wiesner HM, Ugurbil K, Chen W. In vivo measurement of CBF using ^{17}O NMR signal of metabolically produced $H_2{}^{17}O$ as a perfusion tracer. Magn Reson Med. 2013; 70:309–314. [PubMed: 23001743]
40. Chen, W., Zhu, XH., Ugurbil, K. Imaging Cerebral Metabolic Rate of Oxygen Consumption ($CMRO_2$) using ^{17}O NMR Approach at Ultra-high Field. In: Shulman, RG., Rothman, DL., editors. Brain Energetics and Neuronal Activity. John Wiley & Sons Ltd; New York: 2004. p. 125-146.

41. Zhu XH, Chen W. In vivo oxygen-17 NMR for imaging brain oxygen metabolism at high field. Progress in nuclear magnetic resonance spectroscopy. 2011; 59:319–335. [PubMed: 22027341]
42. Zhu XH, Zhang N, Zhang Y, Zhang X, Ugurbil K, Chen W. In vivo ^{17}O NMR approaches for brain study at high field. NMR Biomed. 2005; 18:83–103. [PubMed: 15770611]
43. Gordji-Nejad A, Mollenhoff K, Oros-Peusquens AM, Pillai DR, Shah NJ. Characterizing cerebral oxygen metabolism employing oxygen-17 MRI/MRS at high fields. MAGMA. 2014; 27:81–93. [PubMed: 24337392]
44. de Graaf RA, Brown PB, Rothman DL, Behar KL. Natural abundance ^{17}O NMR spectroscopy of rat brain in vivo. J Magn Reson. 2008; 193:63–67. [PubMed: 18456525]
45. Zhu XH, Liu X, Lu M, Wiesner HM, Ugurbil K, Chen W. In Vivo ^{17}O MR Imaging and Quantification of $CMRO_2$, CBF and OEF in Human Visual Cortex at Rest and during Activation. Proc Intl Soc Mag Reson Med. 2014; 22:3763.
46. Lu M, Zhang Y, Ugurbil K, Chen W, Zhu XH. In vitro and in vivo studies of ^{17}O NMR sensitivity at 9.4 and 16.4 T. Magn Reson Med. 2013; 69:1523–1527. [PubMed: 22777729]
47. Wiesner HM, Balla DZ, Shajan G, Scheffler K, Ugurbil K, Chen W, Uludag K, Pohmann R. ^{17}O relaxation times in the rat brain at 16.4 tesla. Magn Reson Med. 2015
48. Wiesner HM, Pohmann R, Balla DZ, Chen W, Ugurbil K, Uludag K. Measurement of $CMRO_2$ changes by somatosensory stimulation in rat using oxygen-17 at 16.4 T. Proc Intl Soc Mag Reson Med. 2011; 19:1500.
49. Hoult DI, Richards RE. The signal-to-noise ratio of the nuclear magnetic resonance experiment. 1976. J Magn Reson. 2011; 213:329–343. [PubMed: 22152352]
50. Cui W, Zhu XH, Vollmers ML, Colonna ET, Adriany G, Tramm B, Dubinsky JM, Oz G. Non-invasive measurement of cerebral oxygen metabolism in the mouse brain by ultra-high field ^{17}O MR spectroscopy. J Cereb Blood Flow Metab. 2013; 33:1846–1849. [PubMed: 24064490]
51. Lou S, Lepak VC, Eberly LE, Roth B, Cui W, Zhu XH, Oz G, Dubinsky JM. Oxygen consumption deficit in Huntington disease mouse brain under metabolic stress. Human molecular genetics. 2016
52. Mellon EA, Beesam RS, Baumgardner JE, Borthakur A, Witschey WR 2nd, Reddy R. Estimation of the regional cerebral metabolic rate of oxygen consumption with proton detected ^{17}O MRI during precision $^{17}O_2$ inhalation in swine. Journal of neuroscience methods. 2009; 179:29–39. [PubMed: 19428508]
53. Zhu XH, Wiesner HM, Lee BY, Lu M, Chen W. Quantitative and Simultaneous Imaging of $CMRO_2$, CBF and OEF in Resting Human Brain. Proc Intl Soc Mag Reson Med. 2015; 23:895.
54. Borowiak R, Groebner J, Haas M, Hennig J, Bock M. Direct cerebral and cardiac ^{17}O-MRI at 3 Tesla: initial results at natural abundance. MAGMA. 2014; 27:95–99. [PubMed: 24077796]
55. Hoffmann SH, Begovatz P, Nagel AM, Umathum R, Schommer K, Bachert P, Bock M. A measurement setup for direct ^{17}O MRI at 7 T. Magn Reson Med. 2011; 66:1109–1115. [PubMed: 21394777]
56. Hoffmann SH, Radbruch A, Bock M, Semmler W, Nagel AM. Direct ^{17}O MRI with partial volume correction: first experiences in a glioblastoma patient. MAGMA. 2014; 27:579–587. [PubMed: 24687775]
57. Lu M, Atthe B, Mateescu GD, Flask CA, Yu X. Assessing mitochondrial respiration in isolated hearts using ^{17}O MRS. NMR Biomed. 2012; 25:883–889. [PubMed: 22161858]
58. Delapaz R, Gupte P. Potential application of ^{17}O MRI to human ischemic stroke. Adv Exp Med Biol. 2011; 701:215–222. [PubMed: 21445790]
59. Wiesner HM, Luo W, Yang QX, Zhu XH, Schillak S, Chen W. Quantitative Study of TX/RX-efficiency of X-Nuclear MRS/MRI at High/Ultrahigh Field. Proc Intl Soc Mag Reson Med. 2014; 22:810.
60. Qian Y, Stenger VA, Boada FE. Parallel imaging with 3D TPI trajectory: SNR and acceleration benefits. Magnetic resonance imaging. 2009; 27:656–663. [PubMed: 19110392]

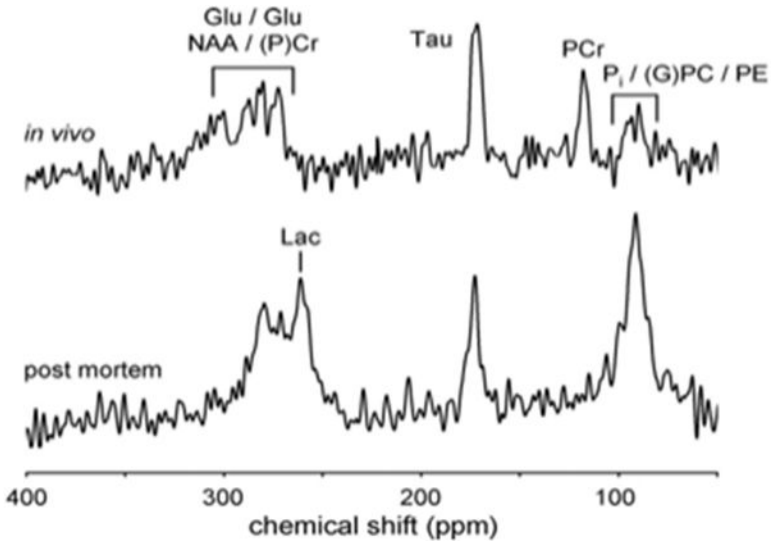

Figure 1.

Pulse-acquired natural abundance ^{17}O MR spectra of rat brain: live (top, 1.5 million averages) and post mortem (bottom, 3.5 million averages) brains obtained with 6 and 14 hours data acquisition, respectively (chemical shifts are referenced to the water signal at 0 ppm). Adapted from reference [44]. Copyright © 2008 Elsevier Inc.

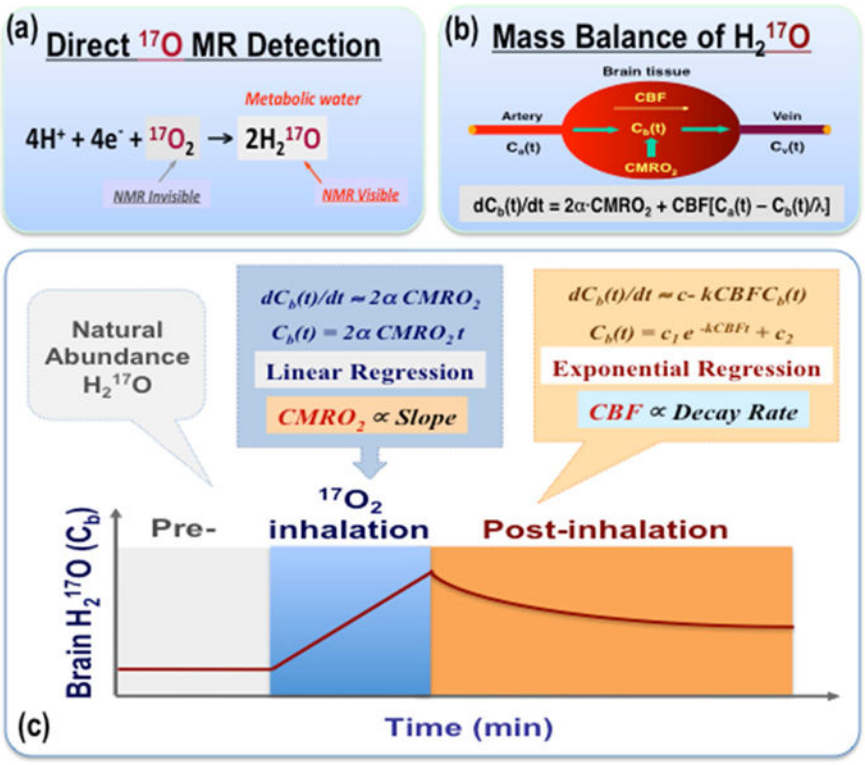

Figure 2.

Schematic illustration of *in vivo* ^{17}O MR technique for quantifying $CMRO_2$ and CBF in rodents *via* a brief inhalation of ^{17}O-labeled oxygen gas: the principle (a), quantification model and mass balance equation (b), as well as the simplified method for calculating $CMRO_2$ and CBF based on the brain $H_2{}^{17}O$ time course (c) are displayed. Detailed description and explanation of the method can be found in references [38–39 & 40–43].

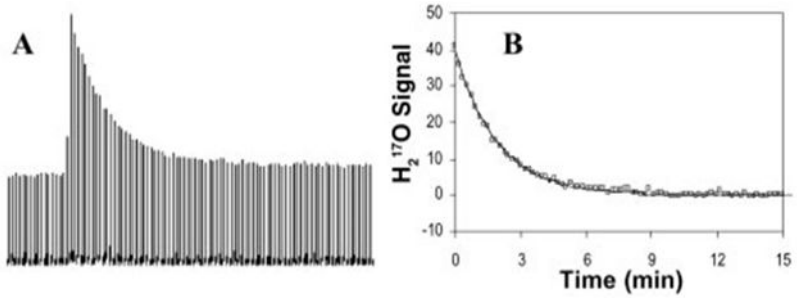

Figure 3.

^{17}O-MR based CBF measurement: (A) stacked plots of the cerebral $H_2{}^{17}O$ spectra after a bolus injection of $H_2{}^{17}O$ into an internal carotid artery of a rat; (B) exponential decay fitting of the $H_2{}^{17}O$ washout curve for calculating CBF. Adapted from reference [26]. Copyright © 2002, National Academy of Sciences, U.S.A.

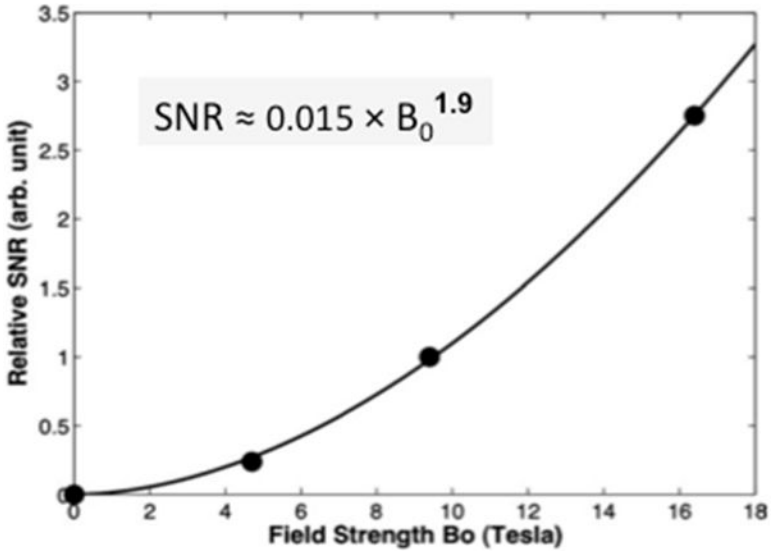

Figure 4.

Field dependence of the relative ^{17}O SNR in the rat brains (filled circles) normalized to the SNR value measured at 9.4. The equation represents the fitting result (solid line) of the experimental data covering the B_0 fields of zero to 16.4 T. Adapt from reference [46].

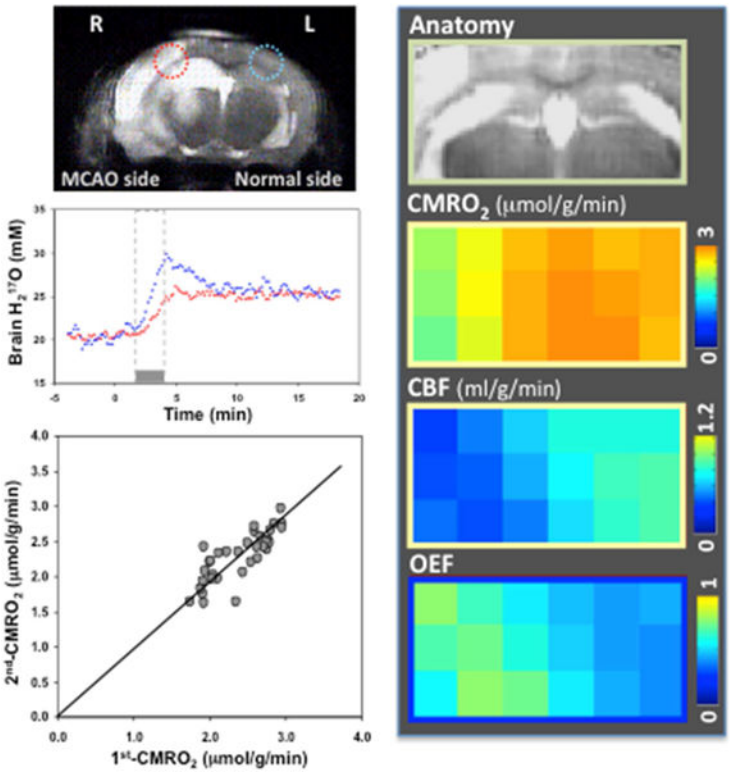

Figure 5.

In vivo ^{17}O MR application in stroke mice: anatomic image with ischemic and intact voxels identified; corresponding dynamic $H_2{}^{17}O$ signals before, during and after a 2-min $^{17}O_2$ inhalation in a mouse model of tMCAo; reproducibility of repeated imaging measurements; and $CMRO_2$, CBF and OEF maps indicating significant changes in ischemia affected brain region. Adapted from reference [38]. Copyright © 2012 Elsevier Inc.

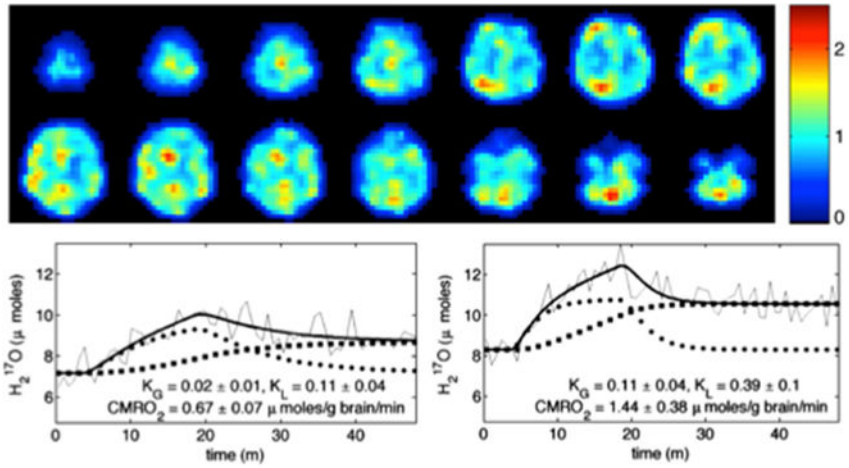

Figure 6.

^{17}O MR based $CMRO_2$ imaging in human brain: $CMRO_2$ maps in mol/g brain/min unit (top) and representative $H_2{}^{17}O$ time-courses for single voxels corresponding to low (bottom left, white matter) and high (bottom right, gray matter) metabolic rates. The three-phase metabolic model of water production (thick line) accurately describes the ^{17}O MR data (thin line) to yield $CMRO_2$ values with K_G and K_L constants shown. Adapted from reference [36].

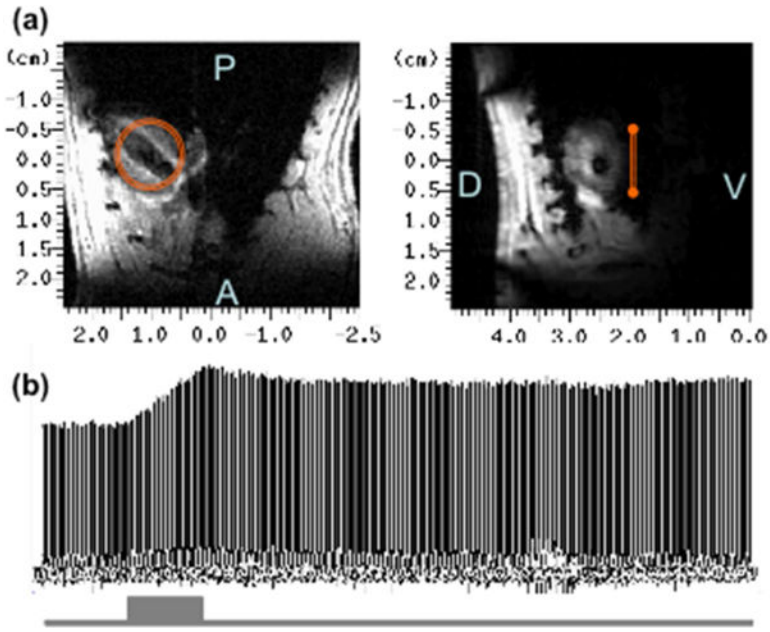

Figure 7.

In vivo ^{17}O MR application in heart: (a) ^{1}H MRI of rat heart in axial (left panel) and sagittal (right panel) orientation showing the ^{17}O surface coil location; (b) stack plot of the heart ^{17}O-water signals acquired before, during (grey bar) and after the inhalation of $^{17}O_2$ gas.